Geophysical Research Letters

RESEARCH LETTER
10.1029/2024GL109137

Multi-Decadal Variability of Amundsen Sea Low Controlled by Natural Tropical and Anthropogenic Drivers

Quentin Dalaiden[1], Nerilie J. Abram[2,3,4,5], Hugues Goosse[1], Paul R. Holland[6], Gemma K. O'Connor[7], and Dániel Topál[1,8]

[1]Earth and Life Institute, Université catholique de Louvain, Louvain-la-Neuve, Belgium, [2]Research School of Earth Sciences, Australian National University, Canberra, ACT, Australia, [3]Australian Centre for Excellence in Antarctic Science, Australian National University, Canberra, ACT, Australia, [4]ARC Centre of Excellence for Climate Extremes, Australian National University, Canberra, ACT, Australia, [5]Centre of Excellence for 21st Century Weather, Australian National University, Canberra, ACT, Australia, [6]British Antarctic Survey, Cambridge, UK, [7]School of Oceanography, University of Washington, Seattle, WA, USA, [8]Institute for Geological and Geochemical Research, HUN-REN Research Centre for Astronomy and Earth Sciences, MTA-Centre of Excellence, Budapest, Hungary

Abstract A crucial factor influencing the mass balance of the West Antarctic Ice Sheet is the Amundsen Sea Low (ASL), a climatological low-pressure region situated off the West Antarctic coast. However, albeit the deepening of the ASL since the 1950s has been attributed to anthropogenic forcing, the multi-decadal variability of the ASL remains poorly understood, because of a lack of long observations. Here, we apply a newly developed data assimilation method to reconstruct the ASL over 1870–2000. We study the forced and internal variability of the ASL using our new reconstruction in concert with existing large ensembles of climate model simulations. Our findings robustly demonstrate that an atmospheric teleconnection originating from the tropical Indo-Pacific is the main driver of ASL variability at the multi-decadal time scale, with resemblance to the Interdecadal Pacific Oscillation. Since the mid-20th century, anthropogenic forcing has emerged as a dominant contributor to the strengthening of the ASL.

Plain Language Summary Changes in the West Antarctic Ice Sheet mass balance (i.e., the difference between the gain and loss of ice mass) are partly influenced by large-scale winds, and in particular, a climatological low-pressure feature located off the West Antarctic coast called the Amundsen Sea Low (ASL). Yet, although the long-term strengthening of the ASL since the mid-20th century has been demonstrated to be related to anthropogenic forcing, our understanding of the variability of the ASL on time-scales of decades is poorly known. In this paper, we therefore investigate the origins of this variability since 1870, and quantify the relative contributions of human-caused climate changes and natural variability of the climate system. For this purpose, we use several ensembles of model simulations as well as new climate reconstructions that combine paleoclimate records with model simulations using a statistical method. Our results indicate that the multi-decadal variability of the ASL is strongly driven by tropical variability in the Indo-Pacific through atmospheric connections between this region and the Amundsen Sea. Our reconstruction, when compared with a large ensemble of model simulations, indicates that since 1950, human-induced climate forcing has become a dominant driver of long-term ASL variability, contributing equally to tropical variability.

Key Points:

- The large-scale atmospheric circulation in West Antarctica exhibits a strong multi-decadal variability superimposed by a 20th-century trend
- The multi-decadal variability of this large-scale atmospheric circulation is strongly governed by the Indo-Pacific tropical variability
- Since 1950, anthropogenic forcing has emerged as a key driver of the long-term change of this atmospheric circulation

Supporting Information:

Supporting Information may be found in the online version of this article.

Correspondence to:

Q. Dalaiden,
quentin.dalaiden@uclouvain.be

Citation:

Dalaiden, Q., Abram, N. J., Goosse, H., Holland, P. R., O'Connor, G. K., & Topál, D. (2024). Multi-decadal variability of Amundsen Sea low controlled by natural tropical and anthropogenic drivers. *Geophysical Research Letters*, *51*, e2024GL109137. https://doi.org/10.1029/2024GL109137

Received 5 MAR 2024
Accepted 31 JUL 2024

Author Contributions:

Conceptualization: Quentin Dalaiden, Nerilie J. Abram, Hugues Goosse
Data curation: Quentin Dalaiden
Formal analysis: Quentin Dalaiden, Nerilie J. Abram, Hugues Goosse, Paul R. Holland, Gemma K. O'Connor
Funding acquisition: Quentin Dalaiden, Nerilie J. Abram, Hugues Goosse
Methodology: Quentin Dalaiden, Nerilie J. Abram, Hugues Goosse, Paul R. Holland
Resources: Quentin Dalaiden, Paul R. Holland
Visualization: Quentin Dalaiden
Writing – original draft: Quentin Dalaiden

1. Introduction

The West Antarctic Ice Sheet (WAIS) offers one of the biggest threats to accelerating global sea level rise in the coming decades (McKay et al., 2022). The WAIS has been losing ice throughout the satellite era (Otosaka et al., 2023), primarily due to changes in the transport of warm ocean waters toward the base of the ice shelves in the Amundsen Sea sector (Pritchard et al., 2012; Shepherd et al., 2004). There is evidence that these changes are driven by local winds, which influence the flow of warm deep waters onto the continental shelf on decadal (Jenkins et al., 2016; Silvano et al., 2022; Steig et al., 2012; Thoma et al., 2008) to centennial (Naughten et al., 2022, 2023) timescales. In West Antarctica the climate, and more specifically surface winds, are strongly controlled by the climatological low-pressure region located off the Amundsen Sea coast (Amundsen Sea Low (ASL) (Hosking et al., 2013; Raphael et al., 2016; Turner et al., 2013). The ASL is not only one of the main drivers of oceanic heat transport toward the ice shelf cavities (Dotto et al., 2020), but it also regulates synoptic-scale weather systems that directly impact the WAIS surface mass balance (SMB) (Hosking et al., 2017) as well as

Writing – review & editing: Quentin Dalaiden, Nerilie J. Abram, Hugues Goosse, Paul R. Holland, Gemma K. O'Connor, Dániel Topál

the sea ice (Hobbs et al., 2024). Hence, analyzing the long-term variability of the ASL is key to understanding changes in both ice shelf melting and in SMB, constraining the WAIS's contribution to future global sea-level rise.

Utilizing 20th century reconstructions (based on ice-core records) (Dalaiden et al., 2021; O'Connor et al., 2021), Dalaiden et al. (2022) suggested that the overall ASL deepening observed over the 1950–2000 period is primarily a forced response to anthropogenic emissions of stratospheric ozone depleting substances and greenhouse gases. However, the origin of the multi-decadal variability of the ASL over the past century is yet to be addressed. In particular, the contribution of internal variability at multi-decadal timescales remains largely unexplored in West Antarctica. This poses a substantial gap in our understanding of how internal variability may mask or enhance externally forced trends, and complicates the interpretation of historical records and the evaluation of future climate risks.

The Interdecadal Pacific Oscillation (IPO) is the dominant internal mode of decadal to multi-decadal sea surface temperature (SST) variability in the Pacific Ocean (Henley et al., 2015; Power et al., 1999) with far-reaching impacts on the Southern Hemisphere high-latitudes (Li et al., 2021). The IPO links multi-decadal SST variability in the tropics with variability in the ASL, similar to atmospheric convection anomalies related to the El Nino Southern Oscillation at interannual timescales; upper-tropospheric convection anomalies trigger stationary Rossby waves, which form a wave train from the tropics to the Amundsen Sea (Lachlan-Cope & Connolley, 2006; Li et al., 2021). Previous studies predominantly analyzed the instrumental period (especially after 1979) when investigating the role of the IPO in influencing surface climate variability over the Antarctic (Chung et al., 2022; Clem et al., 2020; Ding et al., 2011; Li et al., 2014; Meehl et al., 2016; Purich et al., 2016; Turner et al., 2016). As a result, these studies examined year-to-year variability since 1979 but not the multidecadal variability, given that a few decades is inadequate for correctly assessing multidecadal changes. Our study aims at contributing to the understanding of the influence of the multidecadal IPO variability on the ASL by analyzing historical changes back to 1870.

Given the significant influence of large-scale atmospheric dynamic changes on surface climate in West Antarctica and subsequent global climate change impacts, it is crucial to accurately quantify the relative contributions of internal and forced variability in past and future climates for this region (Naughten et al., 2023). Regarding the long-term trend, Dalaiden et al. (2022) demonstrated that the ASL deepening over 1950–2000 is attributed to changes in anthropogenic forcing. Holland et al. (2019) analyzed climate model simulations that were constrained to follow the observed variability in tropical Pacific sea-surface temperatures over the 20th century, allowing them to separate the modeled influence of anthropogenic and tropical forcings respectively on winds over the Amundsen Sea. Using the paleoclimate reconstruction of O'Connor et al. (2021) and additional model simulations, Holland et al. (2022) quantified the relative contributions of internal variability and external forcing to wind changes over the 20th century. Building upon this previous work, here we combine evidence from paleoclimate records and historical climate model simulations to examine the relative contribution of multi-decadal tropical Pacific variability and anthropogenic forcing in regulating the large-scale atmospheric circulation in the West Antarctic sector, specifically the ASL, from 1870. By comparing the reconstructed variability and large ensembles of climate model simulations, we quantify the contribution of internal and forced components in multi-decadal variations of the ASL observed over the 20th century, with particular attention to variability arising from tropical Indo-Pacific teleconnections. Our approach offers a distinct advantage by allowing us to estimate forced variability independently of climate models, mitigating potential biases associated with their forced response. Our analysis thus provides a valuable alternative to previous studies, which relied solely on models for the forced variability.

2. Methodology

In an effort to address variability in the ASL before the instrumental era, we make use of paleoclimate records—especially ice-core and coral records, which allow us to reconstruct climate in the Antarctic and tropics, respectively—and climate model simulations. Specifically, we create new reconstructions of the Southern Hemisphere climate by combining paleoclimate records with climate model physics through an offline paleoclimate data assimilation (DA) method (e.g., Hakim et al., 2016). As described in more detail in Dalaiden et al. (2021), we reconstruct key climate variables at annual resolution from 1870 to 2000 covering the Southern Hemisphere using the isotope-enabled version of the Community Earth System Model version 1 (iCESM1) (Brady et al., 2019; Stevenson et al., 2019) as the DA prior. Overall, it has been demonstrated that CESM typically

performs better than the other ESMs over the Antarctic region (e.g., Agosta et al., 2015; Lenaerts et al., 2016). Additionally, iCESM1 reproduces well the observed spatial variability of precipitation $\delta^{18}O$ over Antarctica (Dütsch et al., 2023). Finally, Figure S1 in Supporting Information S1 indicates that iCESM1 accurately simulates the observed teleconnection from the tropics, including the typical SST pattern in the Pacific and Indian Oceans and the propagation of Rossby waves from the eastern Indian Ocean to the Amundsen Sea. This gives confidence in the use of iCESM1 for our study. The DA method relies on the offline version of a particle filter (van Leeuwen, 2009) that blends the information from observations with a fixed prior estimate of climate variables. In this configuration, the temporal variability of the reconstruction solely comes from the assimilated observations, while the prior propagates the information in space but also to other variables. Therefore, DA-based reconstructions strongly rely on the modeled covariance, which might introduce biases. However, Parsons et al. (2021) have demonstrated that the impact of the biases in the model covariances is much smaller in regions close to the observations that are assimilated. To also reconstruct the tropical variability, here we complement the paleoclimate records used in Dalaiden et al. (2021) (i.e., Antarctic $\delta^{18}O$ and snow accumulation ice-core and tree-ring width records from the mid-to-high latitudes), with tropical coral proxies (see Figure S1 in Supporting Information S1 for the location of all proxies used). All these records are from PAGES2k databases (Stenni et al., 2017a; Thomas et al., 2017a; PAGES2k Consortium, 2013, 2017; Tierney et al., 2015). Additionally, we tested the robustness of our results by using an additional prior, the latest version of CESM (CESM2) (Danabasoglu et al., 2020), which was also shown to have adequate performance in simulating Antarctic surface climate (Dunmire et al., 2022).

Assimilating both high-latitude and tropical records to reconstruct the Southern Hemisphere climate induces important challenges. Wills et al. (2022) showed that none of the models participating in CMIP5/6 simulate the observed SST gradient strengthening between the eastern and central part of the tropical Pacific in synchrony with the Southern Ocean cooling (their Figure 2). This discrepancy suggests that models cannot faithfully reproduce observed trends in these two regions simultaneously. As reconstructing both forced and internal variability using a particle filter-based DA is difficult because of those model biases, we decided to only reconstruct the internal multi-decadal variability, using a new method described below.

2.1. Assessing Internal Variability

We reconstruct historical internal variability by subtracting from the total variability (internal and forced) an estimate of the forced signal, derived from the proxies themselves (see Sections 2.1.1 and 2.1.2). Next, we assimilate this internal variability from proxy into unforced climate model simulations (i.e., the forced variability has been removed from the simulations). This approach ensures that our reconstruction is not influenced by potential model biases in the simulated forced variability. We also expect that DA will compensate for model deficiencies in reproducing the internal variability as DA constrains the model to follow the observed signal provided by proxy records. This method has proven successful in several past studies focusing on decadal to multi-decadal timescales (e.g., Steiger et al., 2018). However, removing the forced component from the records before assimilating them introduces new uncertainties, related to the estimation of this forced variability (see Sections 2.1.1 and 2.1.2).

2.1.1. Tropical and Mid-Latitude Records

Different approaches have been developed to extract internal variability from observations (e.g., Deser & Phillips, 2021). Assuming that the forced variability is associated with a common spatial signal, we follow the approach of Trenberth and Shea (2006) and subtract the regional mean of each proxy variable to isolate the internal part of its historical record. This method thus assumes that forced variability in those quantities is associated with a predominantly spatially uniform signature—such as global warming due to increased greenhouse gas concentrations—while internal variability includes a more pronounced regionally varying component. We use the approach of Trenberth and Shea (2006) for coral and tree-ring width records, which come from regions that are strongly related to the global mean temperature, estimating the forced variability in these proxies by averaging all time-series from the same record type. This is equivalent to assuming the forced variability is uniform across the Indo-Pacific tropics for the coral records, and uniform across the South Pacific subtropics for tree rings (Figure S2 in Supporting Information S1) (Hansen et al., 2010; Wills et al., 2018). Stemming from the relatively small number of records, this estimation of the forced variability however still contains high-frequency variability (Figure S3 in Supporting Information S1) which cannot be explained by changes in the external

forcings. Hence, we further apply a 31-year low-pass filter to get the final estimation of the forced variability (it is worth mentioning that this preserves the global impacts of main modes of climate variability such as El Nino events at high time-frequency). Our results are not sensitive to the length of the low-pass filter applied (tested with 51 and 71-year low-pass filters). To derive the internal variability in each proxy record, the regional estimate of forced variability for each proxy type is then subtracted from each proxy time-series of that type. This approach to estimating the forced and internal variability is further validated by using a large ensemble of model simulations, for which we know the true forced variability (see Sections S1.3 and S1.2 in in Supporting Information S1).

2.1.2. Ice-Core Records

No common trend in Antarctic records has been detected over the 20th century, with large differences between West and East Antarctica (Jones et al., 2016; Medley & Thomas, 2019; Nicolas & Bromwich, 2014; Stenni et al., 2017a). While a forced trend since the mid-20th century is observable in West Antarctica due to the deepening of the ASL, the trend is less clear in East Antarctica, possibly because of the lower signal-to-noise ratio for East Antarctic ice-core records Münch et al. (2016). Consequently, the hypothesis of relatively homogeneous trends in Antarctica that could be estimated from a simple spatial averaging does not seem valid and there is a risk of inaccurately estimating the internal component for high-latitude records using the same methodology for ice-core records as for coral and tree-ring width records. Therefore, a different approach was adopted. Among the main surface climate changes observed over the past decades in the Antarctic region, the clearest signal of anthropogenic forcing is emergent in the atmospheric circulation (Gillett et al., 2008). In particular, Dalaiden et al. (2022) demonstrated that the trend in the ASL index (defined as the mean sea-level pressure over 170–290°E, 75–60°S) over 1950–2000 is caused by external forcings. It is worth noting that this definition of the ASL based upon absolute pressure includes the contributions of both the Southern Hemisphere westerly winds and the cyclonic pattern centered in the Amundsen Sea. Considering that the ASL strongly influences the surface climate over the WAIS (Hosking et al., 2013; Raphael et al., 2016), we estimate the forced component of each ice-core record as being the forced ASL-related signal (i.e., removing the linear trend in each ice-core record associated with anthropogenic forcing through the ASL strengthening). In practise, we subtract the forced ASL-congruent signal for each ice-core records using the estimation of the forced ASL of Dalaiden et al. (2022) (for all details, see Section S1.4 in Supporting Information S1). This methodology keeps in the records the signal associated with the natural variability of the ASL we want to reconstruct.

3. Results and Discussion

3.1. Impact of Assimilating Coral Records on the Skill of Antarctic Reconstruction

Dalaiden et al. (2021) previously reconstructed Antarctic surface variability over the past 200 years using the same DA method as employed in this study but focusing solely on ice-core and mid-latitude tree-ring width records (for an exhaustive evaluation of the reconstruction over Antarctica, see Dalaiden et al. (2021)). We repeat the same DA experiment, but here, we assimilate the paleoclimate records after having removed the estimated anthropogenic forced variability (hereafter referred to as south-iCESM-recon). In our new paleo DA-based reconstruction, we also incorporate coral records (hereafter referred to as all-iCESM-recon). We assessed the reconstruction skill for tropical modes utilizing the ERSSTv5 (Extended Reconstructed SST version 5) data set (Huang et al., 2017a). The R^2 and Coefficient of Efficiency (CE > 0 means that the reconstruction is skillful compared to climatology) are used as skill metrics for the evaluation. The inclusion of coral records in the DA framework enhances the skill in capturing the primary modes of tropical climate variability, as expected (Figure S4 in Supporting Information S1). Comparing all-iCESM-recon with ERSSTv5 over the 1979–2000 period, we find high skill for Niño3.4 and IPO reconstructions, with R^2 values of 0.71 (p-value <0.05; CE = 0.67) and 0.72 (p-value <0.05; CE = 0.70), respectively. It is worth mentioning that the skill is weaker for continental variables and sea-ice extent in the Bellinghausen/Amundsen Sea. Overall, our reconstructions' skill scores are similar to other DA-based products utilizing different proxy types, including coral records (Sanchez et al., 2021; Steiger et al., 2018; Tardif et al., 2019; Zhu et al., 2022).

The inclusion of coral records in the DA has minimal impact on capturing year-to-year variability in the ASL compared to the reconstruction based on mid- and high-latitude records (R^2 = 0.51 [p-value <0.05] vs. 0.49 [p-value <0.05] for all-iCESM-recon and south-iCESM-recon, respectively). However, the impact on sea-ice extent in the Weddell and Ross Seas is noteworthy, with R2 reaching 0.46 (p-value <0.05) and 0.44 (p-value <0.05),

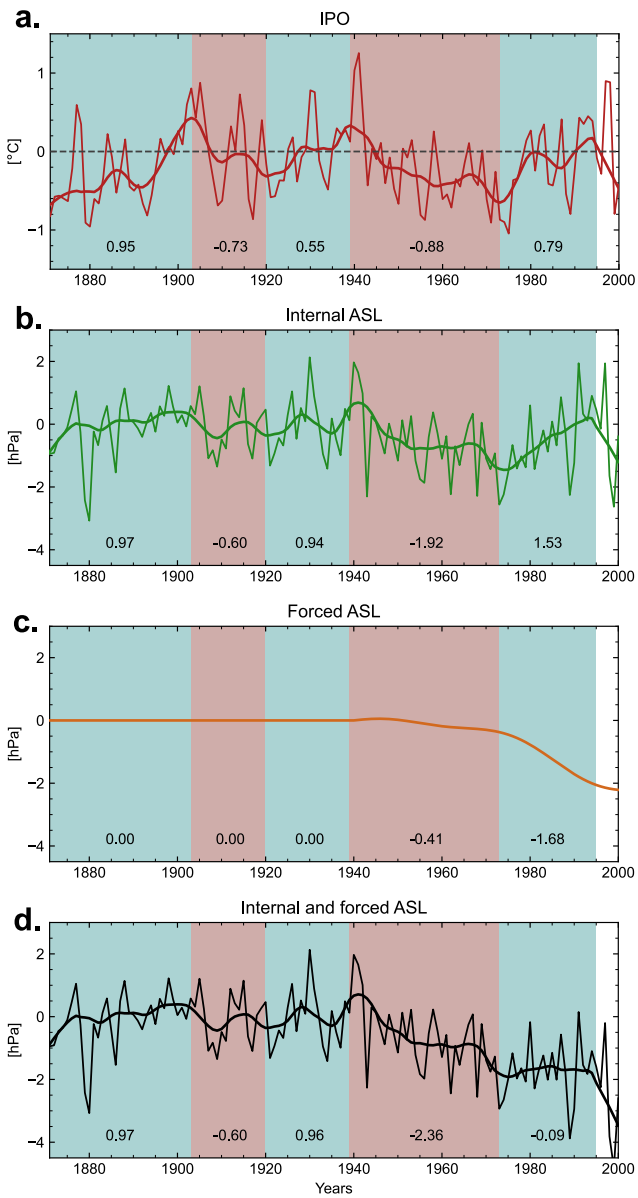

Figure 1. (a–b.) Time-series of the IPO (red; in °C) and internal ASL (green; in hPa) from the natural prior-based reconstruction using all the proxy records (i.e., all-iCESM-recon). (c.) Temporal evolution of the forced ASL computed as the ensemble mean of CESM1-LE (orange; in hPa) scaled to match the observed trend over 1950–2023. (d.) Time-series of the total ASL variability (internal plus forced; black; in hPa). All the time-series are expressed as anomalies relative to the 1901–1930 period. Thick colored lines are moving 13-year averages using lowess smoothing. Periods characterized by declining IPO phases are colored in red while rising IPO phases are in blue. For each period, the difference between the end and the beginning of the anomaly is displayed (based on the 13-year averaged time-series).

respectively for all-iCESM-recon compared to 0.41 (p-value <0.05) and 0.27 (p-value <0.05) for south-iCESM-recon (Figure S4 in Supporting Information S1). This indicates that information from records located in the tropics complements ice-core records when reconstructing historical changes in the West Antarctic climate. This supports the well-established relationship between the tropical and West Antarctic climate variability (Ding et al., 2011; Li et al., 2021; Steig et al., 2012).

The reconstruction based on all the proxies by employing CESM2 as the prior (hereafter referred to as all-CESM2-recon) shares similar features with all-iCESM-recon, in particular a skillful reconstruction of the IPO and ASL. However, the reconstructed variability is weaker in all-CESM2-recon, notably reflected in a reduced CE for the IPO compared with all-iCESM-recon (0.48 vs. 0.68).

3.2. Internal and Forced Components of the ASL Variability Over the 20th Century

Next, we quantify the relative contribution of internal and forced components to the total variability of the ASL. Since our paleo-based reconstruction allows us to only assess the internal variability of the ASL, we need to estimate the forced variability to add it to the internal variability to get the total variability of the ASL. We estimate the ASL forced variability based on the ensemble mean of the single-model initial condition large ensemble CESM1-LE (Kay et al., 2015), and further adjust it to match the observed ASL variability over the 1950–2022 period using a fingerprinting method as in Dalaiden et al. (2022). Utilizing the CESM1-LE ensures consistency in our analysis, given that the all-iCESM-recon is also based on CESM1. Additionally, this estimation of the ASL forced variability is the one used to remove the forced signal from ice-core records. Therefore, by adding this forced variability to the reconstruction of internal variability, this approach ensures a comprehensive representation of variability with proper scaling of the forced variability that is independent of the simulated and reconstructed internal variability.

Figure 1 shows the temporal evolution of the internal (based on all-iCESM-recon), forced and total variability of the ASL, along with the IPO, over the 1870–2000 period. We observe significant multi-decadal variability in the internal ASL, strongly correlated with IPO phases. Indeed, in the all-iCESM-recon, the long-term variability of the internal ASL demonstrates a strong relationship with the IPO at both the annual and multi-decadal timescales over 1870–2000 (r = 0.74 [p-value <0.05] and r = 0.77 [p-value <0.05] when applying a 13-year smoothing, respectively). The all-CESM2-recon also reproduces this strong relation (r = 0.70 [p-value <0.05] and r = 0.79 [p-value <0.05] when applying a 13-year smoothing, respectively; Figure S5 in Supporting Information S1). Although our reconstruction indicates that declining IPO phases systematically lead to a deeper ASL (and vice-versa), the ASL shows no trend between 1870 and 1940 before strongly co-varying with IPO. Hence, it indicates that while the tropical variability—including the IPO—is a key driver of the ASL variability over the past decades, the nature of this relationship may have changed over time (e.g., Dätwyler et al., 2019).

Regarding the total ASL variability, encompassing both internal and forced components, we observe a period characterized by a shallow ASL during 1939–1941 (positive anomaly), which corresponds to an anticyclonic anomaly. From that point onward, the ASL began strengthening until the mid-1970s, remaining relatively stable for approximately two decades before strengthening again around 1990. These variations

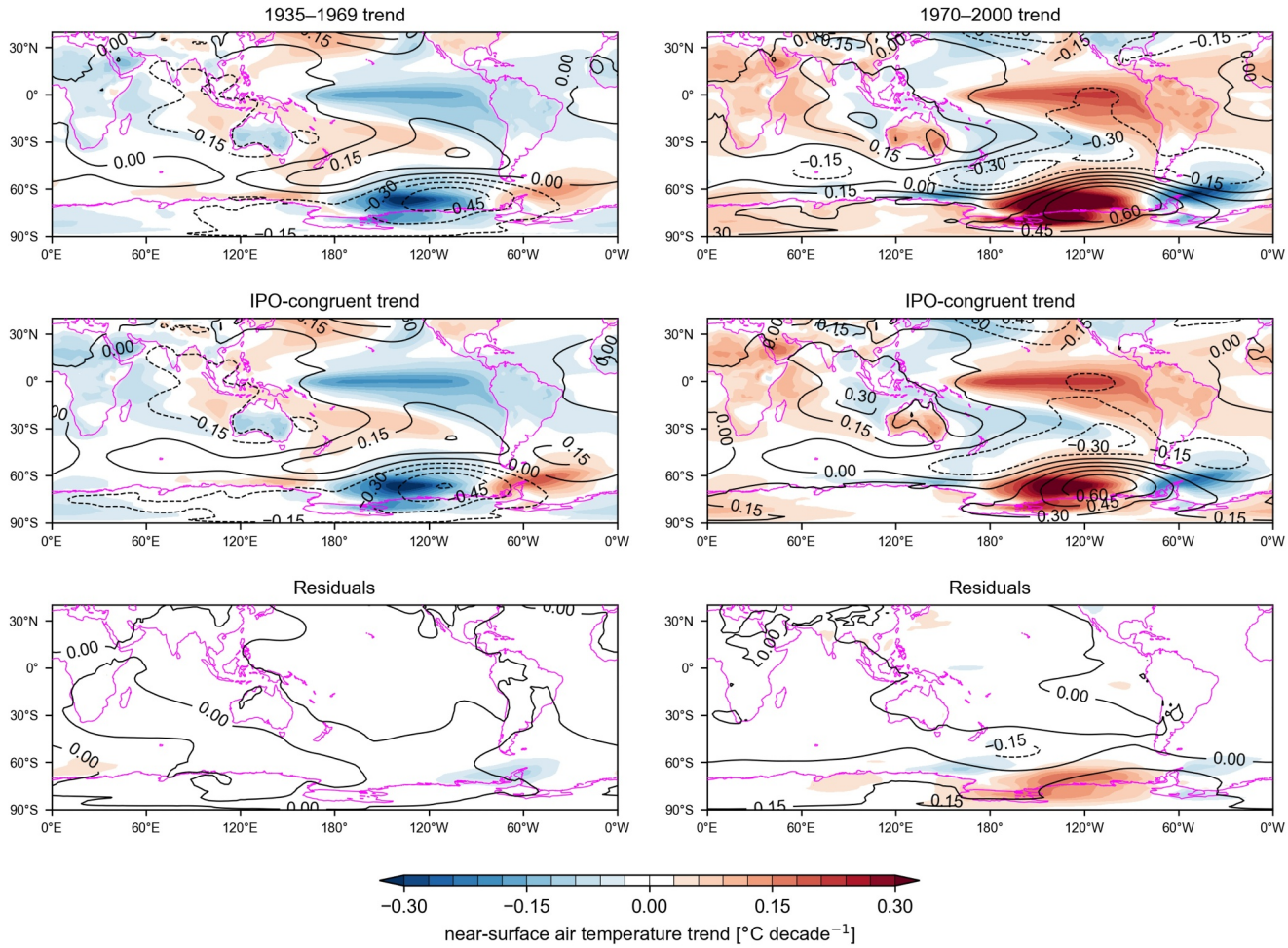

Figure 2. Sea-level pressure (contours; hPa per decade) and sea surface temperature (colors; °C per decade) linear trends in all-iCESM-recon along with the IPO-congruent trends and the residual trend over the 1935–1969 and 1970–2000 periods.

closely align with IPO variability (Figure 1). In the 1939–1941 period, the IPO shifted from a positive to a negative phase, concurrent with intense multi-year El Niño events (Brönnlmann et al., 2004). This may have accounted for the anticyclonic conditions observed in the Amundsen Sea during that period. This is in agreement with the study of O'Connor et al. (2023), which indicates that these anticyclonic conditions result from a combined effect of strong El Niño conditions and other drivers unrelated to tropical Pacific variability. Afterward, the negative IPO phase from around 1940 to the mid-1970s contributed to deepening the ASL.

Subsequently, the IPO shifted to a positive phase in the 1970s. However, unlike previous periods, the ASL remained relatively stable with an apparent slight weakening. During this time, the forced variability exerted a significant influence on the ASL (Figure 1) while, up until the 1970s, ASL variability was predominantly driven by internal processes, displaying minimal influence from anthropogenic forcing. However, from the mid-1970s to the mid-1990s, the internal contribution and the forced contribution exhibited comparable magnitudes but acted in opposite directions, effectively canceling each other out and resulting in a negligible change in the ASL during this period. This illustrates how internal variability can mask forced changes.

3.3. Pacific Tropical Variability as the Main Driver of Multi-Decadal Variability of the ASL

This section aims to investigate the drivers of the internal multi-decadal variability of the ASL, in particular, to quantitatively analyze the role played by tropical forcing. For this purpose, in Figure 2, we analyze the patterns of

SST and sea-level pressure trends in all-iCESM-recon over two distinct periods characterized by the IPO index trending downwards (i.e., 1935–1969; linear trend = −0.20 degC per decade [p-value <0.05]) and upwards (i.e., 1970–2000; linear trend = 0.33 degC per decade [p-value <0.05]). To further analyze the contribution of the IPO variability to these patterns, we computed the SST and sea-level pressure trends associated with IPO by calculating the trends that are linearly congruent with the IPO during the two periods. This is first achieved by computing the sensitivity of SST and sea-level pressure for each grid point to IPO over the 20th century through linear regression (all time-series have been linearly detrended before the calculation). Then, to derive IPO-congruent trends for each grid point, the obtained sensitivity values (i.e., regression coefficients) were multiplied by the linear trend of IPO during the period.

During the 1935–1969 period, the atmospheric circulation pattern indicates negative pressure anomalies all around the Antarctic continent, particularly pronounced in the Amundsen Sea, and positive anomalies in mid-latitudes in the Pacific Sector (Figure 2). This atmospheric pattern is associated with large negative SST anomalies in the Amundsen Sea and positive anomalies from the eastern Antarctic Peninsula to the Weddell Sea. Near the equator, a cyclonic anomaly in the Indian Ocean is apparent. This is a typical atmospheric pattern caused by SST anomalies in the tropical Pacific (Ding & Steig, 2013; Lachlan-Cope & Connolley, 2006; Steig et al., 2012). Anomalous warm water at the surface northwest of Australia induces convection anomalies in the upper troposphere, which in turn triggers the development of a Rossby wave train from the tropics to the Amundsen Sea area (Lachlan-Cope & Connolley, 2006). IPO-congruent trends for both SST and sea-level pressure confirm the pivotal role of IPO in the trends in West Antarctica since almost all of the changes are explained by the IPO. During the 1970–2000 period, positive temperature anomalies were observed in the central Pacific. Although the IPO remains a predominant factor explaining SST and sea-level pressure changes in West Antarctica during this period, the residuals indicate that the influence of the IPO is slightly reduced compared to the 1935–1969 period. These results are also observed in all the reconstructions, regardless of whether the reconstruction includes information from the tropics (coral-iCESM-recon; Figure S6 in Supporting Information S1) or from high/mid-latitudes (south-iCESM-recon; Figure S7 in Supporting Information S1). Therefore, even when tropical records are not included in the DA procedure, the natural way for the climate model to strengthen the ASL is to simulate declining IPO conditions. Of note, we opted declining/inclining IPO over the common negative/positive IPO because, unlike with the phase, the trend informs us about the overall direction of IPO conditions during the period of interest. The covariance also works in the other direction since in the coral-based reconstruction, declining IPO phases are almost systematically associated with an anomalously deep ASL. This strongly suggests that the multi-decadal variability of the ASL is primarily influenced by the multi-decadal variability of the IPO and is not an artifact induced by our methodology. The anthropogenic prior-based reconstruction shows similar results (Figure S8 in Supporting Information S1).

3.4. Origins of the Forced Variability of the ASL

Previous studies indicate that the response of the ASL to external forcing is driven by both stratospheric ozone depletion and greenhouse gas forcing (Dalaiden et al., 2022; Holland et al., 2022). To isolate the impact of the stratospheric ozone depletion and greenhouse gas forcing, we make use of the ensemble of experiments conducted with CESM1 where single forcings were omitted (Deser, Phillips, et al., 2020; Landrum et al., 2017). We compare the simulated ASL in these single-forcing-denied experiments with the forced variability in the full-forcing CESM1-LE (Kay et al., 2015). In order to derive the effects of the forcing, we subtract the single-forcing-denied experiments from the ensemble mean of CESM1-LE (see Deser, Phillips, et al. (2020) for more details). The ensemble without greenhouse-gas forcing includes 20 members, while the ensemble without stratospheric ozone depletion only contains eight members. This therefore leads to a higher variability in the estimated response for the stratospheric ozone depletion. Figure 3 represents the time evolution of the ASL averaged over the three ensembles. Results show that the total forced trend of the ASL over 1970–2000, which reaches −0.35 hPa per decade (p-value <0.05) is equally explained by the two forcings (−0.18 hPa per decade when greenhouse-gas forcing is disabled and −0.17 hPa per decade when stratospheric ozone depletion is disabled). The influence of the forcings on the ASL is especially noticeable from 1970 onwards. The timing thus coincides with the beginning of the rapid forced ASL strengthening at the end of the 20th century (Figure 1).

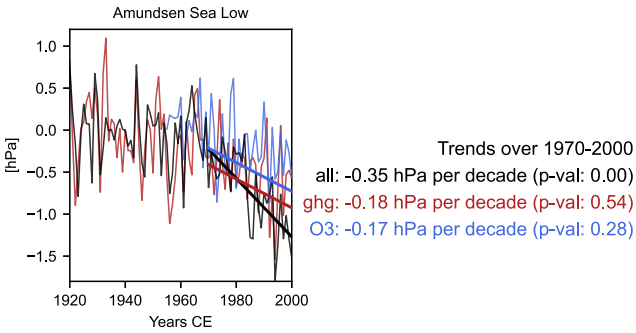

Figure 3. Time-series of simulated ASL response to all forcing (black), greenhouse gas forcing denied (red) and stratospheric ozone depletion denied (blue) ensembles from CESM1-LE (in hPa per decade). The linear trends of the ASL over the 1970–2000 period from the three ensembles are displayed. While the greenhouse gas forcing denied ensemble includes 20 members, the stratospheric ozone depletion denied ensemble only contains eight members. In order to take into account the different ensemble size for the trend significance, we used a bootstrapping method to calculate the p-value of the trend for the greenhouse gas denied ensemble (10,000 iterations by randomly selecting 8 members among the 20 available members).

3.5. Tropical Teleconnections in Climate Models

Since tropical teleconnections have a fundamental role in regulating multi-decadal variability in the South Pacific atmospheric circulation, in Figure 4 we analyze the ASL teleconnections in the models. For this purpose, we analyze the patterns of SST and sea-level pressure during 30-year periods displaying statistically significant (i.e., p-value <0.05) negative or positive trends in the ASL (i.e., ASL strengthening) for the Single-Model Initial condition Large Ensembles (SMILEs) spanning the historical period (Deser, Lehner, et al., 2020). We also include the two tropical Pacemaker ensembles conducted with CESM1 and CESM2 (see Section S1.5 in Supporting Information S1 for more detail). For each SMILE member, we isolate the internal variability by subtracting the ensemble mean of each SMILE and exclude years after 2000 for comparison with the paleo-based reconstruction. In addition to exhibiting widespread negative sea-level pressure anomalies resembling the SAM pattern in comparison with the reconstructions, the models indicate that the multi-decadal variability of the ASL (defined here as a 30-year trend) is not always associated with declining IPO phases (around 70% of the time on average). Although declining IPO phases are observed on average, most models—except for CESM1, CESM2 and CSIRO-Mk-3-6-0—do not simulate the low-pressure system situated in the Indian Ocean as observed in the reconstructions. Therefore, according to the models, the ASL is not exclusively governed by the Indo-Pacific teleconnections. This indicates that models struggle to simulate tropical teleconnections. Indeed, even when only selecting 30-year periods with ASL strengthening and declining IPO phases (Figure S9 in Supporting Information S1), the models still can not reproduce this atmospheric teleconnection. Compared with the Pacific Pacemaker ensemble from CESM1, the Pacific Pacemaker from CESM2 shows an improvement.

4. Conclusions and Implications for Future West Antarctic Climate

In this study, we analyzed the internal and forced variability of the large-scale atmospheric circulation in West Antarctica since 1870 by developing a new method to only assimilate the internal variability from paleo records, on which we added the forced variability estimated from a large ensemble of model simulations. Our findings reveal that tropical teleconnections, in particular the IPO, strongly influence the natural multi-decadal variability of the ASL. However, since about 1950, the variability of the ASL also displays a strong anthropogenic forced trend. Over this period, the magnitude of the internal multidecadal variability is similar to the magnitude of the forced trend so that their interactions can mute or enhance forced changes in the ASL over multidecadal timescales. Our study thus provides additional evidence that West Antarctica is substantially influenced by global climate change. However, owing to the strong internal variability prevailing in the southern high latitudes (e.g., Jones et al., 2016), internal variability has the potential to mask the emergence of the forced climate change trend.

Changes in atmospheric circulation over the Amundsen Sea play a key role in past mass balance variations of the WAIS, encompassing both snow accumulation (Medley & Thomas, 2019) and ice shelf melting (Jenkins et al., 2016; Naughten et al., 2022; Silvano et al., 2022; Steig et al., 2012; Thoma et al., 2008; Verfaillie et al., 2022). Therefore, depending on the phase of the IPO, internal variability could either mitigate the forced response or potentially amplify it to the extent of potentially hastening the destabilization of the WAIS. However, our findings also indicate that state-of-the-art earth system models struggle to accurately reproduce the role of tropical teleconnections in driving changes in the ASL. Open questions remain whether the natural multi-decadal variability of the ASL is governed by factors other than the IPO and whether this teleconnection possesses non-stationary features along with the IPO-ASL connections representation in models.

10.1029/2024GL109137

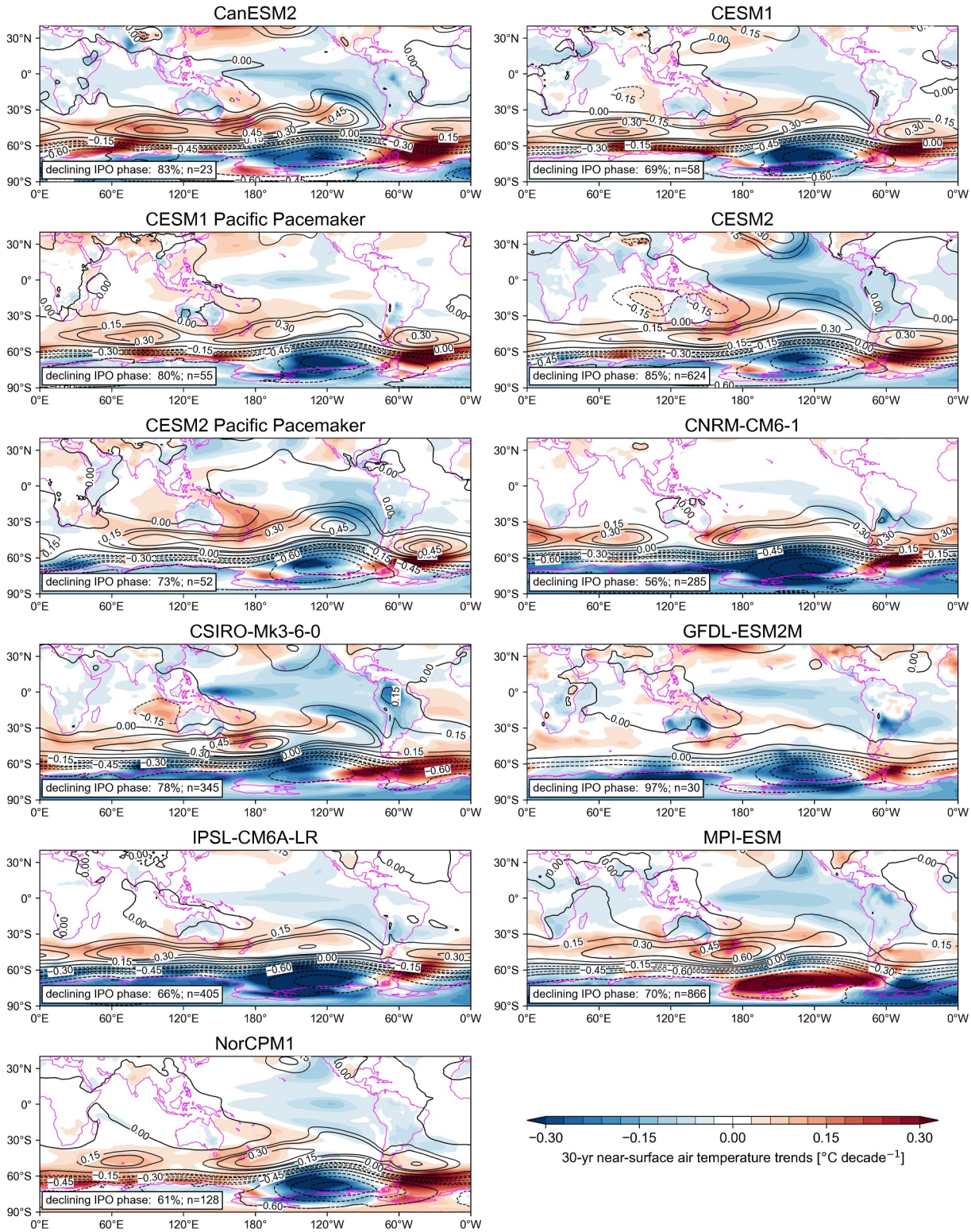

Figure 4. Composites of 30-year trends of SST (colors) and sea-level pressure (contours) during periods displaying 30-year negative statistically significant (p-value <0.05) ASL trends for the SMILEs. The forced variability (estimated as the ensemble mean) is subtracted from each member before building the composites. To increase the sample size, we include 30-year positive statistically significant trends in the composite (and inverting their sign before combining it with the other samples). Both the relative frequency of observed declining IPO phase (in %) and the corresponding sample size are displayed on the map.

Data Availability Statement

CESM outputs are freely available on www.earthsystemgrid.org. Paleoclimate records are accessible through the NOAA World Data Center for Paleoclimatology (Stenni et al., 2017b), British Antarctic Survey website (Thomas et al., 2017b) and *figshare* (Kilbourne et al., 2017). The outputs of the large ensembles are stored on www.earthsystemgrid.org. HadSST and ERSST data sets are available on https://www.metoffice.gov.uk/hadobs/hadsst4/data/download.html and https://psl.noaa.gov/data/gridded/data.noaa.ersst.v5.html (Huang et al., 2017b), respectively.

Acknowledgments
We first would like to thank the two anonymous reviewers for their comments on the study that improved the quality and clarity of the manuscript. Q. D. is a Research Fellow within the F.R.S.-FNRS (Belgium). N. J. Abram was supported by the Australian Research Council Special Research Initiative, Australian Centre for Excellence in Antarctic Science (Project Number SR200100008). H. G. is a Research Director within the F.R.S.-FNRS (Belgium). This study was funded by NERC Grant NE/X000397/1 "Anthropogenic Forcing of Antarctic Ice Loss (AnthroFAIL)." This work was partly performed in the framework of the PDR project T.0101.22 "Role of WINDS and oceanic interactions on Sea ice Changes in the SOuthern Ocean over the Past millennium (WindSCOOP)" of the FRS-FNRS.

References

Agosta, C., Fettweis, X., & Datta, R. (2015). Evaluation of the CMIP5 models in the aim of regional modelling of the Antarctic surface mass balance. *The Cryosphere*, *9*, 2311–2321. https://doi.org/10.5194/tcd-9-3113-2015

Brady, E., Stevenson, S., Bailey, D., Liu, Z., Noone, D., Nusbaumer, J., et al. (2019). The connected isotopic water cycle in the community earth system model version 1. *Journal of Advances in Modeling Earth Systems*, *11*(8), 2547–2566. https://doi.org/10.1029/2019MS001663

Brönnlmann, S., Luterbacher, J., Staehelin, J., Svendby, T. M., Hansen, G., & Svenoe, T. (2004). Extreme climate of the global troposphere and stratosphere in 1940-42 related to El Niño. *Nature*, *431*(7011), 971–974. https://doi.org/10.1038/nature02982

Chung, E.-S., Kim, S.-J., Timmermann, A., Ha, K.-J., Lee, S.-K., Stuecker, M. F., et al. (2022). Antarctic sea-ice expansion and Southern Ocean cooling linked to tropical variability. *Nature Climate Change*, *12*(May), 461–468. https://doi.org/10.1038/s41558-022-01339-z

Clem, K. R., Fogt, R. L., Turner, J., Lintner, B. R., Marshall, G. J., Miller, J. R., & Renwick, J. A. (2020). Record warming at the South Pole during the past three decades. *Nature Climate Change*, *10*(8), 762–770. https://doi.org/10.1038/s41558-020-0815-z

Dalaiden, Q., Goosse, H., Rezsöhazy, J., & Thomas, E. R. (2021). Reconstructing atmospheric circulation and sea-ice extent in the west antarctic over the past 200 years using data assimilation. *Climate Dynamics*, *57*(11), 3479–3503. https://doi.org/10.1007/s00382-021-05879-6

Dalaiden, Q., Schurer, A. P., Kirchmeier-young, M. C., Goosse, H., & Hegerl, G. C. (2022). West antarctic surface climate changes since the mid-20th century driven by anthropogenic forcing geophysical research letters. *Geophysical Research Letters*, *49*(16)e2022GL099543. https://doi.org/10.1029/2022GL099543

Danabasoglu, G., Lamarque, J. F., Bacmeister, J., Bailey, D. A., DuVivier, A. K., Edwards, J., et al. (2020). The community earth system model version 2 (CESM2). *Journal of Advances in Modeling Earth Systems*, *12*(2), 1–35. https://doi.org/10.1029/2019MS001916

Dätwyler, C., Grosjean, M., Steiger, N. J., & Neukom, R. (2019). Teleconnections and relationship between ENSO and SAM in reconstructions and models over the past millennium. *Climate of the Past Discussions*, 1–20. https://doi.org/10.5194/cp-2019-110

Deser, C., Lehner, F., Rodgers, K. B., Ault, T., Delworth, T. L., DiNezio, P. N., et al. (2020a). Insights from Earth system model initial-condition large ensembles and future prospects. *Nature Climate Change*, *10*(4), 277–286. https://doi.org/10.1038/s41558-020-0731-2

Deser, C., & Phillips, A. S. (2021). Defining the internal component of atlantic multidecadal variability in a changing climate. *Geophysical Research Letters*, *48*(22), e2021GL095023. https://doi.org/10.1029/2021GL095023

Deser, C., Phillips, A. S., Simpson, I. R., Rosenbloom, N., Coleman, D., Lehner, F., et al. (2020b). Isolating the evolving contributions of anthropogenic aerosols and greenhouse gases: A new CESM1 large ensemble community resource. *Journal of Climate*, *33*(18), 7835–7858. https://doi.org/10.1175/JCLI-D-20-0123.1

Ding, Q., & Steig, E. J. (2013). Temperature change on the antarctic Peninsula linked to the tropical Pacific. *Journal of Climate*, *26*(19), 7570–7585. https://doi.org/10.1175/JCLI-D-12-00729.1

Ding, Q., Steig, E. J., Battisti, D. S., & Küttel, M. (2011). Winter warming in West Antarctica caused by central tropical Pacific warming. *Nature Geoscience*, *4*(6), 398–403. https://doi.org/10.1038/ngeo1129

Dotto, T. S., Naveira Garabato, A. C., Wåhlin, A. K., Bacon, S., Holland, P. R., Kimura, S., et al. (2020). Control of the oceanic heat content of the getz-dotson trough, Antarctica, by the Amundsen Sea Low. *Journal of Geophysical Research: Oceans*, *125*(8),e2020JC016113. https://doi.org/10.1029/2020JC016113

Dunmire, D., Lenaerts, J. T. M., Datta, R. T., & Gorte, T. (2022). Antarctic surface climate and surface mass balance in the community earth system model version 2 during the satellite era and into the future (1979–2100). *The Cryosphere*, *16*(10), 4163–4184. https://doi.org/10.5194/tc-16-4163-2022

Dütsch, M., Steig, E. J., Blossey, P. N., & Pauling, A. G. (2023). Response of water isotopes in precipitation to a collapse of the west antarctic ice sheet in high-resolution simulations with the weather research and forecasting model. *Journal of Climate*, *36*(16), 5417–5430. https://doi.org/10.1175/JCLI-D-22-0647.1

Gillett, N. P., Stone, D. A., Stott, P. A., Nozawa, T., Karpechko, A. Y., Hegerl, G. C., et al. (2008). Attribution of polar warming to human influence. *Nature Geoscience*, *1*(11), 750–754. https://doi.org/10.1038/ngeo338

Hakim, G. J., Emile-Geay, J., Steig, E. J., Noone, D., Anderson, D. M., Tardif, R., et al. (2016). The last millennium climate reanalysis project: Framework and first results. *Journal of Geophysical Research*, *121*(12), 6745–6764. https://doi.org/10.1002/2016JD024751

Hansen, J., Ruedy, M., Sato, M., & Lo, K. (2010). Global surface temperature change. *Reviews of Geophysics*, *48*(4), 1–29. https://doi.org/10.1029/2010RG000345.1.INTRODUCTION

Henley, B. J., Gergis, J., Karoly, D. J., Power, S., Kennedy, J., & Folland, C. K. (2015). A tripole index for the interdecadal Pacific oscillation. *Climate Dynamics*, *45*(11), 3077–3090. https://doi.org/10.1007/s00382-015-2525-1

Hobbs, W., Spence, P., Meyer, A., Schroeter, S., Fraser, A. D., Reid, P., et al. (2024). Observational evidence for a regime shift in summer antarctic sea ice. *Journal of Climate*, *37*(7), 2263–2275. https://doi.org/10.1175/JCLI-D-23-0479.1

Holland, P. R., Bracegirdle, T. J., Dutrieux, P., Jenkins, A., & Steig, E. J. (2019). West Antarctic ice loss influenced by internal climate variability and anthropogenic forcing. *Nature Geoscience*, *12*(9), 718–724. https://doi.org/10.1038/s41561-019-0420-9

Holland, P. R., O'Connor, G. K., Bracegirdle, T. J., Dutrieux, P., Naughten, K. A., Steig, E. J., et al. (2022). Anthropogenic and internal drivers of wind changes over the amundsen sea, west Antarctica, during the 20th and 21st centuries. *The Cryosphere*, *16*(12), 5085–5105. https://doi.org/10.5194/tc-16-5085-2022

Hosking, J. S., Fogt, R., Thomas, E. R., Moosavi, V., Phillips, T., Coggins, J., & Reusch, D. (2017). Accumulation in coastal West Antarctic ice core records and the role of cyclone activity. *Geophysical Research Letters*, *44*(17), 9084–9092. https://doi.org/10.1002/2017GL074722

Hosking, J. S., Orr, A., Marshall, G. J., Turner, J., & Phillips, T. (2013). The influence of the amundsen-bellingshausen seas low on the climate of West Antarctica and its representation in coupled climate model simulations. *Journal of Climate*, *26*(17), 6633–6648. https://doi.org/10.1175/JCLI-D-12-00813.1

Huang, B., Thorne, P. W., Banzon, V. F., Boyer, T., Chepurin, G., Lawrimore, J. H., et al. (2017a). 09). Extended reconstructed Sea Surface temperature, version 5 (ERSSTv5): Upgrades, validations, and intercomparisons. *Journal of Climate*, *30*(20), 8179–8205. https://doi.org/10.1175/JCLI-D-16-0836.1

Huang, B., Thorne, P. W., Banzon, V. F., Boyer, T., Chepurin, G., Lawrimore, J. H., et al. (2017b). NOAA extended reconstructed Sea Surface temperature (ERSST), version 5 [Dataset]. *NOAA National Centers for Environmental Information*. https://doi.org/10.7289/V5T72FNM

Jenkins, A., Dutrieux, P., Jacobs, S., Steig, E., Gudmundsson, H., Smith, J., & Heywood, K. (2016). Decadal Ocean forcing and Antarctic ice sheet response: Lessons from the Amundsen Sea. *Oceanography*, *29*(4), 106–117. https://doi.org/10.5670/oceanog.2016.103

Jones, J. M., Gille, S. T., Goosse, H., Abram, N. J., Canziani, P. O., Charman, D. J., et al. (2016). Assessing recent trends in high-latitude Southern Hemisphere surface climate. *Nature Climate Change*, *6*(10), 917–926. https://doi.org/10.1038/nclimate3103

Kay, J. E., Deser, C., Phillips, A., Mai, A., Hannay, C., Strand, G., et al. (2015). The community earth system model (CESM) large ensemble project: A community resource for studying climate change in the presence of internal climate variability. *Bulletin of the American Meteorological Society*, *96*(8), 1333–1349. https://doi.org/10.1175/BAMS-D-13-00255.1

Kilbourne, H., Yu, Z., Neukom, R., Nash, D., Gergis, J., Steig, E., et al. (2017). A global multiproxy database for temperature reconstructions of the Common Era. [Collection]. *Figshare*. https://doi.org/10.6084/m9.figshare.c.3285353.v2

Lachlan-Cope, T., & Connolley, W. (2006). Teleconnections between the tropical Pacific and the Amundsen-bellinghausens sea: Role of the El Niño/Southern oscillation. *Journal of Geophysical Research*, *111*(23), 1–10. https://doi.org/10.1029/2005JD006386

Landrum, L. L., Holland, M. M., Raphael, M. N., & Polvani, L. M. (2017). Stratospheric ozone depletion: An unlikely driver of the regional trends in Antarctic sea ice in Austral Fall in the late twentieth century. *Geophysical Research Letters*, *44*(21), 11062–11070. https://doi.org/10.1002/2017GL075618

Lenaerts, J. T., Vizcaino, M., Fyke, J., van Kampenhout, L., & van den Broeke, M. R. (2016). Present-day and future Antarctic ice sheet climate and surface mass balance in the Community Earth System Model. *Climate Dynamics*, *47*(5–6), 1367–1381. https://doi.org/10.1007/s00382-015-2907-4

Li, X., Cai, W., Meehl, G. A., Chen, D., Yuan, X., Raphael, M., et al. (2021). Tropical teleconnection impacts on Antarctic climate changes. *Nature Reviews Earth & Environment*, *2*(10), 680–698. https://doi.org/10.1038/s43017-021-00204-5

Li, X., Holland, D. M., Gerber, E. P., & Yoo, C. (2014). Impacts of the north and tropical Atlantic Ocean on the Antarctic Peninsula and sea ice. *Nature*, *505*(7484), 538–542. https://doi.org/10.1038/nature12945

McKay, D. I. A., Staal, A., Abrams, J. F., Winkelmann, R., Sakschewski, B., Loriani, S., et al. (2022). Exceeding 1.5°c global warming could trigger multiple climate tipping points. *Science*, *377*(6611), eabn7950. https://doi.org/10.1126/science.abn7950

Medley, B., & Thomas, E. R. (2019). Increased snowfall over the Antarctic Ice Sheet mitigated twentieth-century sea-level rise. *Nature Climate Change*, *9*(1), 34–39. https://doi.org/10.1038/s41558-018-0356-x

Meehl, G. A., Arblaster, J. M., Bitz, C. M., Chung, C. T., & Teng, H. (2016). Antarctic sea-ice expansion between 2000 and 2014 driven by tropical Pacific decadal climate variability. *Nature Geoscience*, *9*(8), 590–595. https://doi.org/10.1038/ngeo2751

Münch, T., Kipfstuhl, S., Freitag, J., Meyer, H., & Laepple, T. (2016). Regional climate signal vs. local noise: A two-dimensional view of water isotopes in Antarctic firn at Kohnen station, dronning maud land. *Climate of the Past*, *12*(7), 1565–1581. https://doi.org/10.5194/cp-12-1565-2016

Naughten, K. A., Holland, P. R., & De Rydt, J. (2023). Unavoidable future increase in West Antarctic ice-shelf melting over the twenty-first century. *Nature Climate Change*, *13*(11), 1222–1228. https://doi.org/10.1038/s41558-023-01818-x

Naughten, K. A., Holland, P. R., Dutrieux, P., Kimura, S., Bett, D. T., & Jenkins, A. (2022). Simulated twentieth-century ocean warming in the Amundsen Sea, West Antarctica. *Geophysical Research Letters*, *49*(5), e2021GL094566. https://doi.org/10.1029/2021GL094566

Nicolas, J. P., & Bromwich, D. H. (2014). New reconstruction of antarctic near-surface temperatures: Multidecadal trends and reliability of global reanalyses. *Journal of Climate*, *27*(21), 8070–8093. https://doi.org/10.1175/JCLI-D-13-00733.1

O'Connor, G. K., Holland, P. R., Steig, E. J., Dutrieux, P., & Hakim, G. J. (2023). Characteristics and rarity of the strong 1940s westerly wind event over the Amundsen sea, west antarctica. *The Cryosphere*, *17*(10), 4399–4420. https://doi.org/10.5194/tc-17-4399-2023

O'Connor, G. K., Steig, E. J., & Hakim, G. J. (2021). Strengthening southern Hemisphere westerlies and Amundsen Sea Low deepening over the 20th century revealed by proxy-data assimilation. *Geophysical Research Letters*, *48*(24). https://doi.org/10.1029/2021gl095999

Otosaka, I. N., Shepherd, A., Ivins, E. R., Schlegel, N.-J., Amory, C., van den Broeke, M. R., et al. (2023). Mass balance of the Greenland and Antarctic ice sheets from 1992 to 2020. *Earth System Science Data*, *15*(4), 1597–1616. https://doi.org/10.5194/essd-15-1597-2023

PAGES2k Consortium. (2013). Continental-scale temperature variability during the past two millennia. *Nature Geoscience*, *6*(5), 339–346. https://doi.org/10.1038/ngeo1797

PAGES2k Consortium. (2017). A global multiproxy database for temperature reconstructions of the Common Era. *Scientific Data*, *4*(July), 170088. https://doi.org/10.1038/sdata.2017.88

Parsons, L. A., Amrhein, D. E., Sanchez, S. C., Tardif, R., Brennan, M. K., & Hakim, G. J. (2021). Do multi-model ensembles improve reconstruction skill in paleoclimate data assimilation? *Earth and Space Science*, *8*(4), e2020EA001467. https://doi.org/10.1029/2020EA001467

Power, S., Casey, T., Folland, C., Colman, A., & Mehta, V. (1999). Inter-decadal modulation of the impact of ENSO on Australia. *Climate Dynamics*, *15*(5), 319–324. https://doi.org/10.1007/s003820050284

Pritchard, H. D., Ligtenberg, S. R., Fricker, H. A., Vaughan, D. G., Van Den Broeke, M. R., & Padman, L. (2012). Antarctic ice-sheet loss driven by basal melting of ice shelves. *Nature*, *484*(7395), 502–505. https://doi.org/10.1038/nature10968

Purich, A., England, M. H., Cai, W., Chikamoto, Y., Timmermann, A., Fyfe, J. C., et al. (2016). Tropical pacific SST drivers of recent antarctic sea ice trends. *Journal of Climate*, *29*(24), 8931–8948. https://doi.org/10.1175/JCLI-D-16-0440.1

Raphael, M. N., Marshall, G. J., Turner, J., Fogt, R. L., Schneider, D., Dixon, D. A., et al. (2016). The Amundsen sea low: Variability, change, and impact on Antarctic climate. *Bulletin of the American Meteorological Society*, *97*(1), 111–121. https://doi.org/10.1175/BAMS-D-14-00018.1

Sanchez, S. C., Hakim, G. J., & Saenger, C. P. (2021). Climate model teleconnection patterns govern the niño-3.4 response to early nineteenth-century volcanism in coral-based data assimilation reconstructions. *Journal of Climate*, *34*(5), 1863–1880. https://doi.org/10.1175/JCLI-D-20-0549.1

Shepherd, A., Wingham, D., & Rignot, E. (2004). Warm ocean is eroding west antarctic ice sheet. *Geophysical Research Letters*, *31*(23). https://doi.org/10.1029/2004GL021106

Silvano, A., Holland, P. R., Naughten, K. A., Dragomir, O., Dutrieux, P., Jenkins, A., et al. (2022). Baroclinic ocean response to climate forcing regulates decadal variability of ice-shelf melting in the Amundsen sea. *Geophysical Research Letters*, *49*(24), e2022GL100646. https://doi.org/10.1029/2022GL100646

Steig, E. J., Ding, Q., Battisti, D. S., & Jenkins, A. (2012). Tropical forcing of circumpolar deep water inflow and outlet glacier thinning in the Amundsen sea embayment, west Antarctica. *Annals of Glaciology*, *53*(60), 19–28. https://doi.org/10.3189/2012AoG60A110

Steiger, N. J., Smerdon, J. E., Cook, E. R., & Cook, B. I. (2018). A reconstruction of global hydroclimate and dynamical variables over the Common Era. *Scientific Data*, *5*, 1–15. https://doi.org/10.1038/sdata.2018.86

Stenni, B., Curran, M. A., Abram, N. J., Orsi, A., Goursaud, S., Masson-Delmotte, V., et al. (2017b). NOAA/WDS paleoclimatology - PAGES Antarctica2k temperature reconstructions [Dataset]. *NOAA National Centers for Environmental Information*. https://doi.org/10.25921/h6nr-kt92

Stenni, B., Curran, M. A., Abram, N. J., Orsi, A., Goursaud, S., Masson-Delmotte, V., et al. (2017a). Antarctic climate variability on regional and continental scales over the last 2000 years. *Climate of the Past*, *13*(11), 1609–1634. https://doi.org/10.5194/cp-13-1609-2017

Stevenson, S., Capotondi, A., Fasullo, J., & Otto-Bliesner, B. (2019). Forced changes to twentieth century ENSO diversity in a last Millennium context. *Climate Dynamics*, *52*(12), 7359–7374. https://doi.org/10.1007/s00382-017-3573-5

Tardif, R., Hakim, G. J., Perkins, W. A., Horlick, K. A., Erb, M. P., Emile-Geay, J., et al. (2019). Last millennium reanalysis with an expanded proxy database and seasonal proxy modeling. *Climate of the Past*, *15*(4), 1251–1273. https://doi.org/10.5194/cp-15-1251-2019

Thoma, M., Jenkins, A., Holland, D., & Jacobs, S. (2008). Modelling circumpolar deep water intrusions on the Amundsen Sea continental shelf, Antarctica. *Geophysical Research Letters*, *35*(18), 2–7. https://doi.org/10.1029/2008GL034939

Thomas, E. R. (2017b). Antarctic regional snow accumulation composites over the past 1000 years - Version 2 (Version 2.0) [Dataset]. *Polar Data Centre, Natural Environment Research Council, UK*. https://doi.org/10.5285/cc1d42de-dfe6-40aa-a1a6-d45cb2fc8293

Thomas, E. R., Melchior Van Wessem, J., Roberts, J., Isaksson, E., Schlosser, E., Fudge, T. J., et al. (2017a). Regional Antarctic snow accumulation over the past 1000 years. *Climate of the Past*, *13*(11), 1491–1513. https://doi.org/10.5194/cp-13-1491-2017

Tierney, J. E., Abram, N. J., Anchukaitis, K. J., Evans, M. N., Giry, C., Kilbourne, K. H., et al. (2015). Tropical sea surface temperatures for the past four centuries reconstructed from coral archives. *Paleoceanography*, *30*(3), 226–252. https://doi.org/10.1002/2014PA002717

Trenberth, K. E., & Shea, D. J. (2006). Atlantic hurricanes and natural variability in 2005. *Geophysical Research Letters*, *33*(12),L12704. https://doi.org/10.1029/2006GL026894

Turner, J., Phillips, T., Hosking, J. S., Marshall, G. J., & Orr, A. (2013). The Amundsen sea low. *International Journal of Climatology*, *33*(7), 1818–1829. https://doi.org/10.1002/joc.3558

Turner, J., Scott Hosking, J., Marshall, G. J., Phillips, T., & Bracegirdle, T. J. (2016). Antarctic sea ice increase consistent with intrinsic variability of the Amundsen sea low. *Climate Dynamics*, *46*(7–8), 2391–2402. https://doi.org/10.1007/s00382-015-2708-9

van Leeuwen, P. J. (2009). Particle filtering in geophysical systems. *Monthly Weather Review*, *137*(12), 4089–4114. https://doi.org/10.1175/2009MWR2835.1

Verfaillie, D., Pelletier, C., Goosse, H., Jourdain, N. C., Bull, C. Y. S., Dalaiden, Q., et al. (2022). The circum-Antarctic ice-shelves respond to a more positive Southern Annular Mode with regionally varied melting. *Communications Earth & Environment*, *3*(1), 139. https://doi.org/10.1038/s43247-022-00458-x

Wills, R. C., Dong, Y., Proistosecu, C., Armour, K. C., & Battisti, D. S. (2022). Systematic climate model biases in the large-scale patterns of recent sea-surface temperature and sea-level pressure change. *Geophysical Research Letters*, *49*(17), e2022GL100011. https://doi.org/10.1029/2022GL100011

Wills, R. C., Schneider, T., Wallace, J. M., Battisti, D. S., & Hartmann, D. L. (2018). Disentangling global warming, multidecadal variability, and el niño in pacific temperatures. *Geophysical Research Letters*, *45*(5), 2487–2496. https://doi.org/10.1002/2017GL076327

Zhu, F., Emile-Geay, J., Anchukaitis, K. J., Hakim, G. J., Wittenberg, A. T., Morales, M. S., et al. (2022). A re-appraisal of the ENSO response to volcanism with paleoclimate data assimilation. *Nature Communications*, *13*(1), 1–10. https://doi.org/10.1038/s41467-022-28210-1

References From the Supporting Information

Capotondi, A., Deser, C., Phillips, A. S., Okumura, Y., & Larson, S. M. (2020). ENSO and Pacific decadal variability in the community earth system model version 2. *Journal of Advances in Modeling Earth Systems*, *12*(12). https://doi.org/10.1029/2019MS002022

Cavitte, M., Dalaiden, Q., Goosse, H., Lenaerts, J., & Thomas, E. (2020). Reconciling the surface temperature–surface mass balance relationship in models and ice cores in Antarctica over the last two centuries. *The Cryosphere*, *14*, 4083–4102. https://doi.org/10.5194/tc-2020-36

Conroy, J. L., Thompson, D. M., Cobb, K. M., Noone, D., Rea, S., & Legrande, A. N. (2017). Spatiotemporal variability in the δ^{18}o-salinity relationship of seawater across the tropical pacific ocean. *Paleoceanography*, *32*(5), 484–497. https://doi.org/10.1002/2016PA003073

Dee, S., Emile-Geay, J., Evans, M. N., Allam, A., Steig, E. J., & Thompson, D. (2015). Prysm: An open-source framework for proxy system modeling, with applications to oxygen-isotope systems. *Journal of Advances in Modeling Earth Systems*, *7*(3), 1220–1247. https://doi.org/10.1002/2015MS000447

Dee, S. G., Cobb, K. M., Emile-geay, J., Ault, T. R., Edwards, R. L., Cheng, H., & Charles, C. D. (2020). No consistent ENSO response to volcanic forcing over the last millennium. *Science*, *367*(6485), 1477–1481. https://doi.org/10.1126/science.aax2000

Dubinkina, S., Goosse, H., Sallaz-Damaz, Y., Crespin, E., & Crucifix, M. (2011). Testing a particle filter to reconstruct climate changes over the past centuries. *International Journal of Bifurcation and Chaos*, *21*(12), 3611–3618. https://doi.org/10.1142/S0218127411030763

Evans, M. N., Tolwinski-Ward, S. E., Thompson, D. M., & Anchukaitis, K. J. (2013). Applications of proxy system modeling in high resolution paleoclimatology. *Quaternary Science Reviews*, *76*, 16–28. https://doi.org/10.1016/j.quascirev.2013.05.024

Franke, J., Valler, V., Brönnimann, S., Neukom, R., & Jaume-Santero, F. (2020). The importance of input data quality and quantity in climate field reconstructions – Results from the assimilation of various tree-ring collections. *Climate of the Past*, *16*(3), 1061–1074. https://doi.org/10.5194/cp-16-1061-2020

Kennedy, J. J., Rayner, N. A., Atkinson, C. P., & Killick, R. E. (2019). An ensemble data set of sea surface temperature change from 1850: The met office hadley centre hadsst.4.0.0.0 data set. *Journal of Geophysical Research: Atmospheres*, *124*(14), 7719–7763. https://doi.org/10.1029/2018JD029867

Klein, F., Abram, N. J., Curran, M. A. J., Goosse, H., Goursaud, S., Masson-Delmotte, V., et al. (2019). Assessing the robustness of Antarctic temperature reconstructions over the past two millennia using pseudoproxy and data assimilation experiments. *Climate of the Past*, *15*, 661–684. https://doi.org/10.5194/cp-2018-90

Milinski, S., Maher, N., & Olonscheck, D. (2020). How large does a large ensemble need to be? *Earth System Dynamics*, *11*(4), 885–901. https://doi.org/10.5194/esd-11-885-2020

Oger, S., Sime, L., & Holloway, M. (2023). Decoupling of δ^{18}o from surface temperature in Antarctica in an ensemble of historical simulations. *EGUsphere, 2023*, 1–29. https://doi.org/10.5194/egusphere-2023-2735

Parkinson, C. L. (2019). A 40-y record reveals gradual Antarctic sea ice increases followed by decreases at rates far exceeding the rates seen in the Arctic. *Proceedings of the National Academy of Sciences of the United States of America*, *116*(29), 14414–14423. https://doi.org/10.1073/pnas.1906556116